RESEARCH ARTICLE

Modulating the Differentiation of Kinetically Controlled Supramolecular Polymerizations through the Alkyl Bridge Length

Cristina Naranjo,[a] Sergio Adalid,[a] Rafael Gómez,[a] and Luis Sánchez*[a]

Dedicated to Professor Enrique Ortí on the occasion of his 65th birthday

[a] C. Naranjo, S. Adalid, Dr. R. Gómez, Prof. Dr. L. Sánchez
Departamento de Química Orgánica, Facultad de Ciencias Químicas
Universidad Complutense de Madrid
Ciudad Universitaria, s/n; 28040-Madrid (Spain)
E-mail: crisnara@ucm.es; sergiada@ucm.es; rafaelgomez@quim.ucm.es; lusamar@ucm.es

Supporting information for this article is given via a link at the end of the document.

Abstract: The synthesis and self-assembling features of N-annulated perylenebisimides (N-PBIs) **2-4** are reported and compared with the complex self-assembly of N-PBI **1**. The studies presented herein demonstrate that increasing the length of the alkyl spacer separating the central aromatic core of the dye and the peripheral side chains cancels the differentiation on the corresponding supramolecular polymerization. Thus, only **2** is able form two different supramolecular polymorphs. The formation of kinetically trapped monomeric species is observed for all the N-PBIs **2-4**. These metastable species, constituted by intramolecularly H-bonded pseudocycles of 7, 8, 9 or 10 members for compounds **1**, **2**, **3** and **4**, respectively, provoke kinetically controlled supramolecular polymerizations that can be accelerated by the addition of seeds. The results presented herein shed light on the intricate process of differentiation in self-assembly.

Introduction

The self-assembly pathways shown by biomolecules afford complex systems displaying different structures and functions. As a consequence, adaptability and diversity emerge as striking characteristic of these supramolecular systems. These pathways stem from complex energy landscapes that these systems go across until they reach the thermodynamic equilibrium.[1] The kinetics of this pathway complexity is a key issue in these processes and, therefore, understanding the kinetics of the self-assembly is a crucial point. Pathway complexity in supramolecular chemistry, and more specifically in supramolecular polymers, has emerged as a powerful benchmark to mimic the natural processes followed by biomolecules to yield complex, functional structures.[2,3] Contrary to those supramolecular polymers organized under thermodynamic control, that are formed either through isodesmic or (anti)cooperative supramolecular polymerization mechanisms,[3] kinetically controlled supramolecular polymerization can give rise to more complex situations in which on-pathway and off-pathway aggregated species are formed in a consecutive or a competitive manner by the appearance of metastable species (*M**) that retard the supramolecular polymerization event.[2,4,5] Importantly, the seminal example of seeded supramolecular polymerization of Sugiyasu, Takeuchi and coworkers paved the way to programmable self-assembly events yielding functional, aggregated species of controlled polydispersity.[6] The entrapment of the monomeric species into metastable states by the operation of intramolecular H-bonding interactions is often present in kinetically controlled supramolecular polymerizations. The addition of seeds, attained from thermodynamically controlled aggregated species, to these metastable monomers accelerates the formation of such thermodynamically controlled supramolecular polymers.[7]

However, pathway complexity brought to light more complex, but still scarcely understood, processes in which a single monomeric species affords more than two aggregated species. This phenomenon, termed *differentiation*,[8] has been reported for the three different luminescent aggregates formed by Pt^{II} complexes,[9] the 1D or 2D aggregates yielded by zinc porphyrins,[8] or the three 1D supramolecular polymorphs formed by perylenebisimides (PBIs) endowed with chiral side chains.[10] Our research group reported on the outstanding self-assembling features shown by N-annulated perylenebisimides (N-PBIs) decorated with trialkoxybenzamide fragments which, depending on the experimental conditions, are able to form up to four aggregated species, three J-type and one H-type aggregated species, giving rise to a complex energy landscape.[11]

To study in more detail the potential differentiation experienced in the supramolecular polymerization of N-PBIs, herein we report on the synthesis of a series of these dyes (compounds **1-4** in Figure 1) in which the alkyl bridge separating the N-PBI core and the trialkoxybenzamide moieties increases in length ranging from two, that corresponds to the previously reported N-PBI **1**,[11] up to five methylene units. These systematic studies, that demonstrate the influence of the linker connecting the central aromatic units and the peripheral side chains in kinetically controlled supramolecular studies, even if limited,[12] are relevant to stablish structure-function rules in the field. The spectroscopic and microscopy studies carried out on N-PBIs **1-4** reveal that increasing the length of the alkyl bridge reduces the differentiation phenomenon. Thus, **1** is able to form up to four supramolecular polymorphs,[11] N-PBI **2**, with an alkyl bridge of three methylenes, forms only two different aggregated species but **3** and **4**, endowed with linkers with four and five methylene units, respectively, yield only one

aggregated species despite the higher conformational freedom of the central alkyl bridge. Unlike N-PBI **1,** that forms charge-transfer (CT) mediated J-type aggregates,[13] the self-assembly of all the new N-PBIs **2-4** affords H-type aggregates. Finally, the presence of the trialkoxybenzamide moiety attached to the N-annulated perylene unit by a linear spacer of a varying number of methylene units allows the formation of an intramolecularly H-bonded pseudocycle that retards the corresponding supramolecular polymerization (Figure 1). This process can be accelerated by the addition of seeds. The results presented herein help in establishing a structure–function in kinetically controlled supramolecular polymerizations and shed light on the intricate process of differentiation in self-assembly.

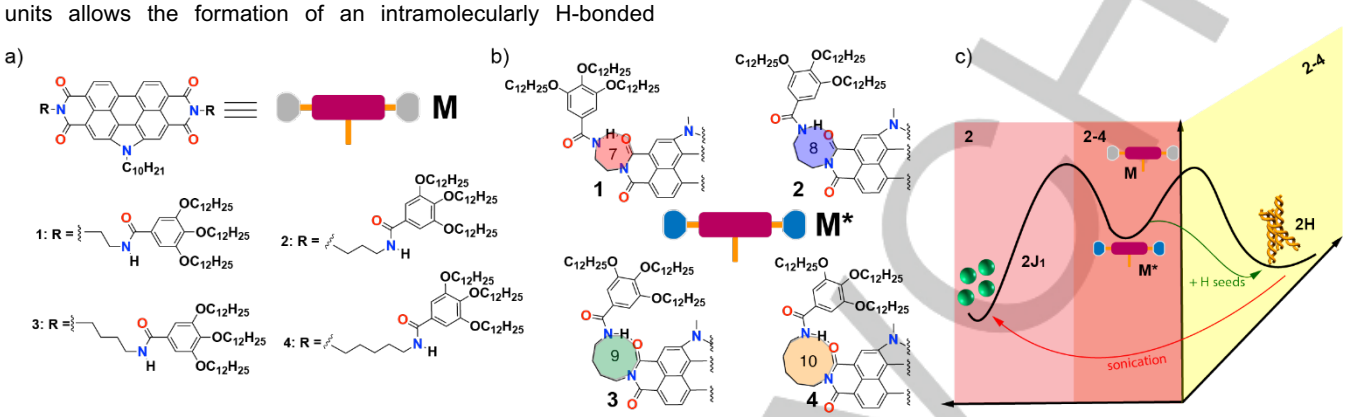

Figure 1. Chemical structure of the N-annulated PBIs **1–4** showing the open arms (a) and the metastable 7–10-membered pseudocycles (b); (c) Illustration of the self-assembling processes taking place with compounds **2**-**4**. The red part represents the formation of the metastable monomeric species detected for all **2-4**; the yellow part depicts the formation of the kinetically controlled formation of the fibrillar aggregates for N-PBIs **2-4,** that can be accelerated by the addition of seeds, and the pink part shows the formation of the nanoparticles upon sonication of the fibrillar aggregates of compound **2**. All these species have been detected in MCH/Tol 1/1 mixtures as solvent.

Results and Discussion

Synthesis and supramolecular polymerization. As it was in the case of compound **1**,[11] N-PBIs **2-4** were synthesized in a multistep protocol starting from commercially available perylene-3,4,9,10-tetracarboxylic dianhydride, methyl 3,4,5-trihydroxybenzoate and propane-1,3-diamine, putrescine, and cadaverine for **2**, **3**, and **4**, respectively (for details on synthesis and characterization, see the Electronic Supporting Information, ESI).

To investigate the supramolecular polymerization mechanism and the non-covalent forces operating in the self-assembly of the reported N-PBIs **2-4**, we have utilized a number of spectroscopic and microscopy techniques and solvents. It is important to remark that the experiments carried out with compounds **2-4** at diluted conditions clearly indicate that chloroform acts a good solvent, thus favoring the presence of molecularly dissolved state, but MCH acts a bad solvent and strongly favors their aggregation. Initially, we have registered concentration dependent ^{1}H NMR spectra to qualitatively unravel the packing of the monomeric species in the aggregated species. Compound **2** shows a negligible shift of the amide protons upon increasing the concentration, diagnostic of the lack of intermolecular H-bonding interactions between the amide functional groups. In addition, a noticeable shielding effect is observed for the aromatic resonances that implies the π-stacking of the aromatic units upon increasing the concentration (Figure S1). Unlike **2**, compounds **3** and **4**, show the shielding of all aromatic resonances and the downfield shift of the amide protons upon increasing the concentration in $CDCl_3$ as solvent (Figures S2 and S3). This behaviour coincides with that observed for NPBIs **1**.[11] These shifts are diagnostic of the π-stacking of the aromatic backbones accompanied by the formation of H-bonding arrays between the amide functional groups. In addition, the upfield shift experienced for the methylene protons constitutive of the alkyl bridge upon increasing the concentration imply the van der Waals interaction of these linkers in the aggregated state (Figure S1-S3).[14] This effect is more noticeable in deuterated toluene (Tol-d8) as solvent. In this deuterated solvent, the ^{1}H NMR spectra at room temperature show very broad bands diagnostic of the formation of oligomeric assemblies that become sharper upon increasing the temperature (Figure 2).

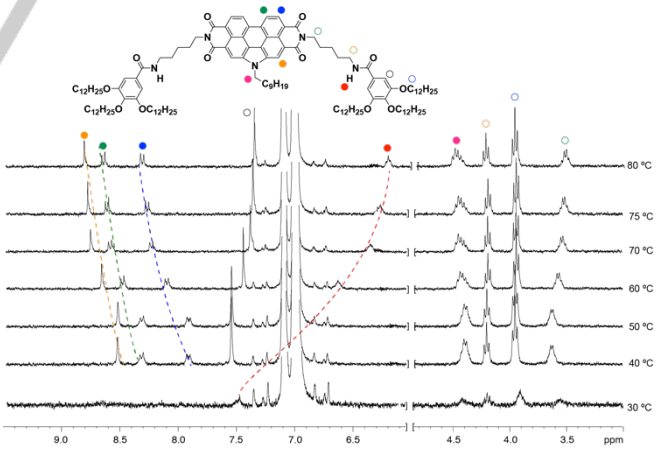

Figure 2. VT-^{1}H NMR spectra of **4** in Tol-d8 (300 MHz, c_T = 1 mM) showing the signals associated to the aromatic protons and to the methylene units linked to the nitrogen and oxygen atoms. The dotted lines depict the shift of the aromatic and amide protons upon increasing the temperature.

In addition, similar shifts to those observed in the concentration dependent ^{1}H NMR experiments carried out in $CDCl_3$ are observed for the aromatic resonances and the amide protons that corroborates the supramolecular interaction of the reported

systems by the π-stacking of the aromatic moieties and the formation of intermolecular H-bonding arrays between the amide functional groups (Figures 2, S4 and S5).[15]

The relevance of the H-bonding interactions to generate the supramolecular polymers from compounds **2-4** has been demonstrated by registering the corresponding FTIR spectra in methylcyclohexane (MCH) or toluene (Tol) as solvents. These apolar solvents strongly favor the organized self-assembly of the investigated systems. In good agreement with many other supramolecular polymers formed by the operation of H-bonding arrays between amide functional groups, the stretching NH and Amide I bands appear at ~3300 and ~1635 cm^{-1} (Figure 3a and S6).[10,12,14] These wavenumber values contrast with those observed in $CHCl_3$, a good solvent that favors the molecularly dissolved state. In this good solvent, NH and Amide I stretching bands appear at ~3450 and ~1655 cm^{-1} (Figure 3a and S6).[10,12,14]

A detailed investigation of the supramolecular polymerization mechanism has been performed by utilizing variable temperature (VT) UV-Vis spectroscopy in MCH as solvent. Noteworthy, these VT-UV-Vis studies carried out with NPBI **1** showed the formation of up to three *J*-type aggregated species.[11] In the case of **2-4**, pristine MCH could not be used since, unlike **1**, heating up the diluted solutions of these N-PBIs up to 90 ºC did not result in the characteristic UV-Vis spectra ascribable to perylene-based monomeric species with two intense bands at λ = 486 and 519 nm, corresponding to the $A_{0\text{-}1}/A_{0\text{-}0}$ transitions[16], *i. e.* **2-4** are in their aggregated states in MCH. To decrease the high stability of the aggregated species formed by **2-4**, we have utilized a MCH/Tol 1/1 mixture as solvent. It is worth mentioning that, in these solvent conditions, compound **1** is able to form four different aggregates species, too.[11]

In the case of compound **2**, heating up a MCH/Tol 1/1 diluted solution at total concentration c_T = 10 μM to 90 ºC results in the complete disassembly of the aggregated species, as demonstrates the absorption pattern of the corresponding UV-Vis spectrum (Figure 3b and S8a). In this solvent mixture and at 20 ºC, the absorption pattern of **2** shows a broad but red-shifted absorption band (λ = 549 nm) in comparison to the absorption pattern exhibited by the monomeric species (λ = 529 nm). This bathochromic shift could be ascribable to the formation of *J*-type aggregates mediated by a partial charge transfer (Figures 3b and S8a).[11 13,18] This partial charge transfer has been reported to play a relevant role in the optical properties of PBI-based self-assemblies.[19] In fact, the emission spectrum of this aggregated species of compound **2** is comparable in shape and intensity to that registered in the same experimental conditions (MCH/Tol, 1/1; 20 ºC, c_T = 20 μM) for the thermodynamically controlled *J*-type aggregates of compound **1** (Figure S7). Noteworthy, both compounds **1** and **2** present an identical emission spectra pattern in $CHCl_3$ that is ascribable to the monomeric species (Figure S7). The differentiation process observed in **1** is achieved by modifying the experimental conditions utilized to afford the aggregated species. Thus, depending of applying a temperature quenching, aging the sample or applying ultrasounds it is possible to detect two additional *J*-type supramolecular polymorphs and one *H*-type polymorph, respectively.[11] In the case of N-PBI **2**, the temperature quenching or the aging process does not result in new supramolecular polymorphs as demonstrate the corresponding UV-Vis spectra that are identical to that recorded in freshly prepared samples (Figure 3b and S8a). However, the sonication of the freshly prepared solution for 15 min yields a new red-shifted absorption pattern that does not change with time (Figure 3b and S8a). These UV-Vis studies reveal that in the case of N-PBI **2**, endowed with three methylene units in the alkyl bridge, it is possible to achieve only two different supramolecular polymorphs.

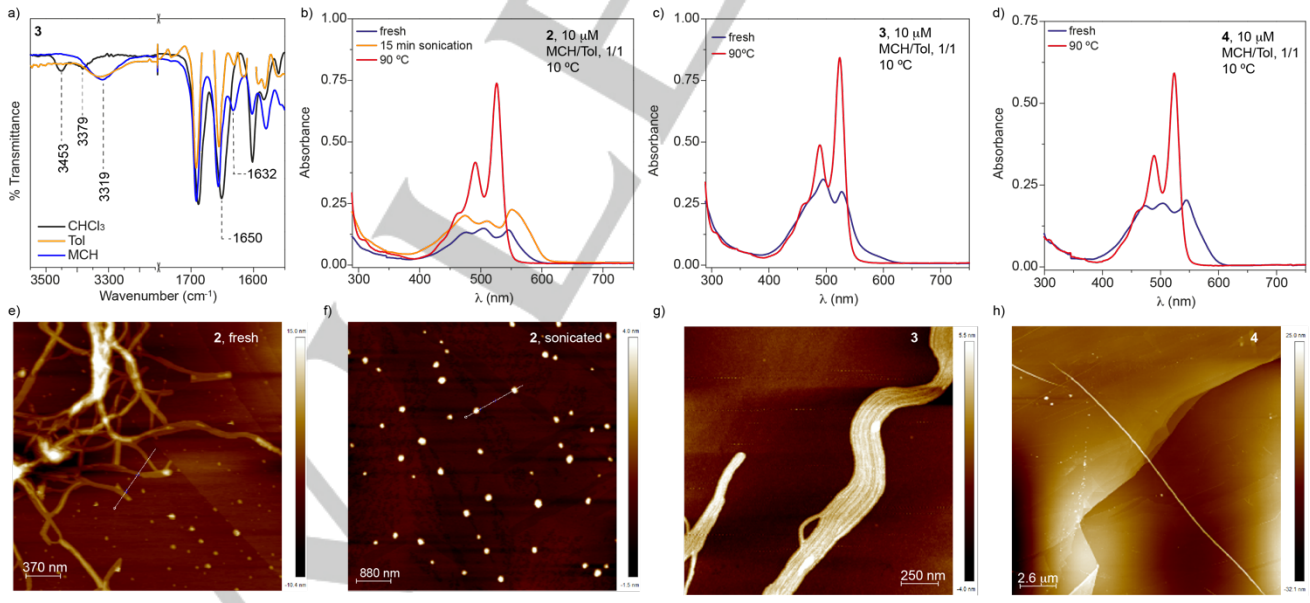

Figure 3. a) Partial FTIR spectra of **3** in solution at c_T = 1 mM in different solvents showing the region in which the N–H stretching and Amide I bands are observed; b-d) UV-Vis spectra of compounds **2-4** in different experimental conditions (MCH/Tol 1/1 as solvent; c_T = 10 μM); e-f) AFM images of the aggregated species formed by N-PBIs **2-4** (experimental conditions. HOPG as surface; MCH/Tol, 1/1 as solvent; c_T = 10 μM).

The dissimilar UV-Vis pattern observed for the freshly and sonicated species obtained for self-assembled **2** results also in different morphology. Atomic force microscopy (AFM) imaging of a spin-coated solution of a fresh sample of compound **2** in MCH/Tol 1/1, at c_T = 10 μM onto highly oriented pyrolytic graphite (HOPG) shows the presence of intertwined fibers with heights of

~ 5 nm (Figure 3e and S9). The AFM images of the sonicated solution, however, show the formation of homogeneous nanoparticles with typical heights of ~ 5 nm (Figure 3f and S9).

N-PBIs **3** and **4**, in which the trialkoxybenzamide fragments are connected to the central *N*-annulated PBI core by four and five methylene units, respectively, show an identical absorption pattern for the molecularly dissolved species with maxima at λ = 491 and 526 nm (Figure 3c, 3d, S8b and S8c). However, the aggregated species of these compounds, observed in MCH/Tol 1/1, at c_T = 10 μM and at 20 ºC, present dissimilar UV-Vis spectra. Thus, compound **3** displays a clear hypochromic effect upon aggregation with maxima at λ = 494 and 527 nm, values very similar to that observed for the monomeric species (Figure 3c and S8b). The supramolecular polymers formed from compound **4** present an UV-Vis spectrum very similar to that observed for N-PBI **2** with maxima at λ = 476, 504 and 546 nm (Figure 3d and S8c). Interestingly, the emission spectra of the aggregated species formed from **3** and **4** experience a clear quenching of the emission intensity in comparison to that observed for the molecularly dissolved species and also in comparison to those registered for the self-assembled aggregates of **1** and **2** (Figure S7c and S7d). An efficient intermolecular charge transfer between the stacked molecular units, resulting of a better packing between these units, could be responsible for the deactivation of the emissive properties of these compounds.

Importantly, changing the experimental conditions by applying a temperature quenching, aging the sample or applying sonication results in no variation in the absorption pattern of the aggregates formed from **3** and **4** which implies that the longer alkyl bridges cancel the differentiation and no additional supramolecular polymorphs are formed from these two N-PBIs **3** and **4** (Figure S8b and S8c).

AFM images of the supramolecular polymers formed by **3** and **4** reveal the fibrillar nature of these aggregated species (Figures 3g, 3h, S10 and S11). However, clear differences are observed in the morphology. Thus, whilst a clear bundling effect of the fibers is observed for the supramolecular polymers formed by **3** (Figure 3g and S10), isolated thick fibers, with typical heights of 20 nm are observed for the aggregates of N-PBI **4** (Figure 3h and S11). This thickness implies the entangling of several thinner fibers to yield rope-like supramolecular structures.

Upon identifying the spectroscopic features of the supramolecular polymers formed by compounds **2-4**, we tried to investigate the supramolecular polymerization mechanism by developing variable temperature (VT) UV-Vis experiments. Heating up diluted solutions (c_T = 10 μM) of **2-4** in MCH/Tol yields the molecularly dissolved state as demonstrates the characteristic absorption pattern (Figure 3b-d and S8). Cooling down this diluted solution until 20 ºC yields a non-sigmoidal curve that could be diagnostic of a cooperative supramolecular polymerization. However, and unlike compound **1**, these non-sigmoidal cooling curves could not be fitted to the one-component equilibrium (EQ) model to derive the thermodynamic parameters associated to the supramolecular polymerization.[20] These cooling curves show that the temperatures of elongation, T_e, that corresponds to the temperatures at which the nuclei start growing to form the aggregated species, is much lower for compounds **2** and **4** (T_e ~ 20 and 25 ºC, respectively), than those observed for **3** (T_e ~ 58 ºC). These T_e values demonstrate that the stability of the supramolecular polymers formed by compounds **2** and **4** is much lower than that exhibited for the N-PBI **3** (Figure 4).

The fact that the above-mentioned cooling curves cannot be fitted to the EQ model, and the previous results reported for **1**, is diagnostic of the operation of a kinetically controlled supramolecular polymerization of N-PBIs **2-4**.[2] That is corroborated by the clear hysteresis observed upon registering the corresponding heating curves. In this case, the temperatures of elongation, T_e', upon heating a 10 μM solution of **2-4,** are much higher than those observed in the cooling curves and more similar for all the three **2-4** (T_e' ~ 68, 75 and 59 ºC, respectively) (Figure 4a-c). The kinetically controlled supramolecular polymerization is accounted for by the formation of metastable monomeric species with 7-, 8-, 9- or 10-membered intramolecular H-bonded pseudocycles (M* in Figure 1b). The formation of these pseudocycles is experimentally demonstrated by the appearance of N-H stretching bands at wavenumbers of around 3400 cm^{-1} in the FTIR spectra recorded in chloroform (Figure 3a and S6)[10-12] and by the VT-^{1}H NMR experiments performed in $CDCl_3$, a good solvent that favors the complete disassembly of the aggregated species. In these VT-^{1}H NMR experiments, carried out for **2-4**, only the triplet corresponding to the amide protons shift upfield upon increasing the temperature, due to the rupture of the intramolecular H-bonding interaction to afford the completely free molecularly dissolved species, whilst neither the aromatic nor the aliphatic resonances experience any change in the chemical shift, since both the completely free monomeric species, M, and the pseudocycles, M*, are not interacting by the π-stacking of the aromatic moieties (Figures S12-14).[7,12]

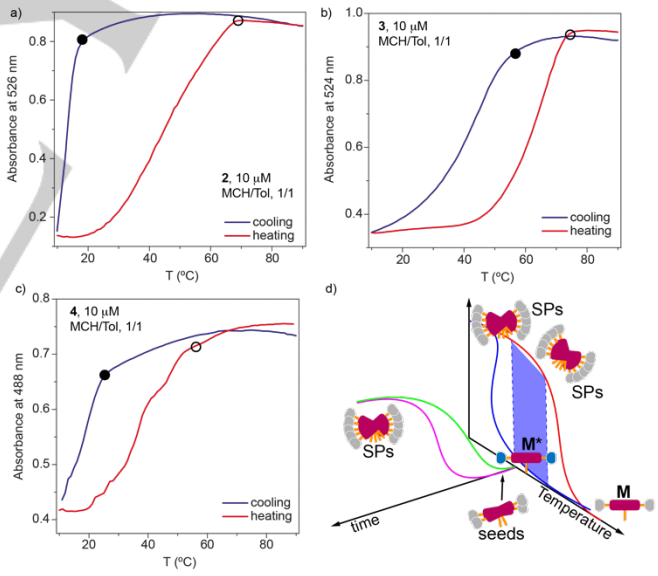

Figure 4. (a-c) Plot of the variation of the absorbance versus temperature by cooling (blue lines) or heating (red lines) at 1 ºC/min diluted solutions of **2** (a), **3** (b) and **4** (c) (experimental conditions: MCH/Tol 1/1; c_T = 10 μM). The solid and hollow circles represent the T_e and T_e' respectively. Panel (d) displays a schematic illustration of the species present at different temperatures upon heating or cooling the samples and the corresponding kinetic profiles without and with seeding. The blue area represents the temperature range at which it is possible to achieve both the metastable monomeric or the aggregated species depending on the heating or cooling cycle.

Seeded supramolecular polymerization. The hysteresis observed in the cooling and heating curves of compounds **2-4** implies that in the range of temperatures encompassing the T_e

and T_e' values it is possible to attain both the metastable monomeric species or the supramolecular polymers (blue region in Figure 4d). Consequently, in this temperature range it is possible to bias the kinetically controlled supramolecular polymerization of the reported N-PBIs by the addition of seeds that can accelerate the conversion of the metastable monomeric species M* into the supramolecular polymers.[7,11] Herein, we have investigated the kinetics of the self-assembly of compounds **2** and **4**; the high T_e value of **3** prevents to accomplish an accurate study of the kinetically controlled process.

To evaluate the kinetics of the supramolecular polymerization of **2**, a 10 μM solution of this N-PBI in MCH/Tol 1/1 is heated up to 90 ºC to achieve a complete disassembly (Figure 5a). After that, this solution is rapidly (10 K/min) cooled down to 25 ºC to form the metastable species M* that are fully converted into the supramolecular polymers in 70 min (Figure 5b). The sigmoidal shape of this kinetics reveals an autocatalytic process that is notably accelerated both by decreasing the temperature (Figure 5b) or by increasing the concentration (Figure 5c). Interestingly, the kinetically controlled supramolecular polymerization of N-PBI **2**, can be strongly accelerated by performing a seeding supramolecular polymerization (SSP). This SSP can be accomplished by preparing seeds of the two different aggregated species formed by N-PBI **2**, i. e. the fibers and nanoparticles. Both types of seeds were prepared by applying different sonication times. Thus, applying only 5 min of sonication to a 10 μM solution of **2** in MCH/Tol 1/1, produces fibrillar seeds. Adding an aliquot of these seeds (1/100 ratio) provokes the conversion of the metastable monomeric species into the supramolecular polymorph with an absorption pattern that coincides with that observed for the freshly prepared aggregate. This conversion is very fast and the lag phase observed in the unseeded kinetic experiment is completely cancelled. However, the sonication of a 10 μM solution of **2** in MCH/Tol 1/1 for more than 20 min affords seeds of the nanoparticle supramolecular polymorph (Figure 5a and 5d). The addition of these seeds to the metastable monomeric species accelerates the conversion of the M* species affording a supramolecular aggregate that presents an absorption pattern coincident with that of the freshly prepared aggregate (Figure 5a and 5d). Therefore, regardless the seed utilized to accelerate the conversion of the metastable monomeric species of compound **2**, the seeded supramolecular polymerization of this N-PBI yields the initially detected supramolecular polymer.

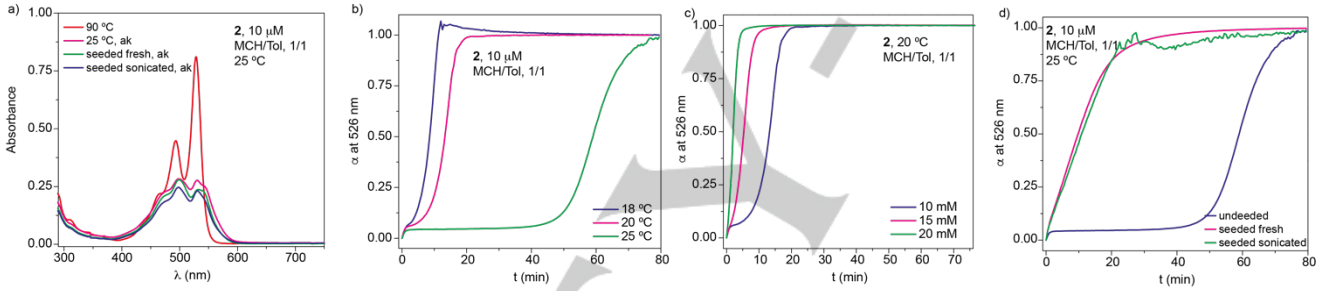

Figure 5. a) UV-Vis spectra of **2** at different temperatures and experimental conditions (ak = after kinetics); b-d) kinetic profiles of the conversion of the metastable monomeric species M* of **2** at different temperatures (b), at different concentrations (c) and upon adding seed of the freshly prepared supramolecular species and the sonicated supramolecular species (d) (experimental conditions: MCH/Tol, 1/1 as solvent; c_T = 10 μM).

The kinetics of the supramolecular polymerization of N-PBI **4** has been evaluated in a similar manner to that described for compound **2**. Taking into account the hysteresis observed in the heating and cooling curves (Figure 4c), we heated up a diluted solution of **4** in MCH/Tol 1/1 to achieve the complete disassembly. After that, we cooled it down to 20 ºC and registered the variation of the degree of aggregation α with time. The kinetic profile of the conversion of the metastable monomeric species M* of **4** also presents a sigmoidal shape characteristic of an autocatalytic process (Figure S15a). However, in this case, the lag phase is much lower than for compound **4** which indicates a faster conversion of M* to produce the corresponding supramolecular polymers. In good agreement with compound **2**, the conversion of the metastable monomeric units of **4** is accelerated upon increasing the concentration (Figure S15b). Finally, and in order to perform the corresponding SSP, we prepared seeds of the supramolecular polymers by sonicating a solution of **4** in MCH/Tol 1/1 at 20 ºC for 10 min. The kinetically trapped monomers are transformed very rapidly, around 10 min, to the corresponding supramolecular polymers upon adding the seed at 1/100 seed/monomer ratio (Figure S15c). In addition, the conversion is also accelerated by applying a much lower seed/monomer ratio (1/500, Figure S15c). In this case, the conversion of the kinetically trapped monomeric species is completed in less than 15 min.

To shed light on the morphology of both the seeds utilized for the SSP of compound **4** and also the supramolecular polymers formed upon this SSP, we have registered AFM images. Upon sonication a diluted solution of **4** in MCH/Tol for 10 min to form the seeds, we have spin-coated an aliquot of this solution onto HOPG. The AFM images shows the formation of isolated, small nanoparticles with height of around 1.5 nm (Figure 6 and S16). Following a similar protocol to that describe above for the SSP polymerization of **4**, we have added these seeds to a previously heated and cooled solution of compound **4** to form the corresponding metastable monomeric species. Upon adding the seeds and after 10 min, we achieved an absorption pattern ascribable to the aggregated species (Figure S15c). An aliquot of these supramolecular polymers has been spin-coated onto HOPG and the AFM images registered. In good correlation with the unseeded samples, the AFM images of the supramolecular polymers formed upon SSP also present the formation of long and intertwined rope-like aggregates with typical heights of ~10 nm (Figure 6 and S17).

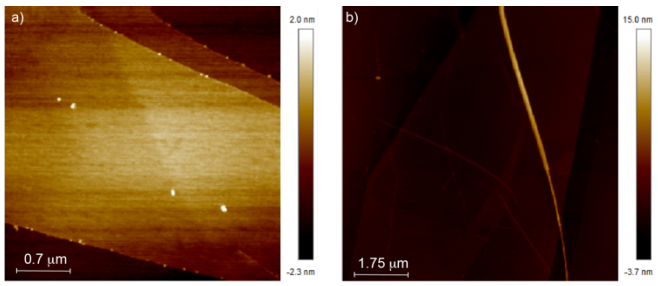

Figure 6. AFM images of the seeds formed upon sonication a diluted solution of **4** (a) and the fibrillar supramolecular polymers formed upon the seeded supramolecular polymerization of **4** (experimental conditions: HOPG as surface; c_T = 10 µM; MCH/Tol 1/1 as solvent).

Conclusion

In this manuscript a detailed investigation on the differentiation experienced in the supramolecular polymerization of N-annulated perylenebisimides (N-PBIs) **1-4**, a series of N-PBIs in which the alkyl bridge separating the central aromatic core and the trialkoxybenzamide moieties increases in length is addressed. The synergy between spectroscopic and microscopy studies reveals that increasing the length of the alkyl bridge reduces the differentiation phenomenon: whilst compound **1**, with an alkyl spacer of two methylenes, is able to form up to four supramolecular polymorphs, increasing the length of the spacer in compound **2** allows unraveling the formation of two different supramolecular polymorphs, the first one being an emissive aggregate with fibrillar morphology that upon sonication yields a second polymorph that self-assembles as nanoparticles. Further increasing the length of the spacer in compounds **3** and **4** cancels the differentiation and the formation of just fibrillar aggregates is detected. Importantly, the peripheral trialkoxybenzamides attached to the imide scaffold is able to form kinetically trapped monomeric species by means of intramolecular H-bonding interactions that affords pseudocycles of 7, 8, 9 or 10 members for compounds **1**, **2**, **3** or **4**, respectively. In good analogy to compound **1**, a seeded supramolecular polymerization has been carried out with N-PBIs **2** and **4** to accelerate the conversion of such metastable monomeric species into the final supramolecular polymers. In short, we demonstrate that longer alkyl spacers separating the peripheral side chains and the central aromatic core of N-PBIs cancels the differentiation. The results presented herein help in establishing a structure–function relationship in kinetically controlled supramolecular polymerizations and shed light on the intricate process of differentiation in self-assembly.

Acknowledgements

Financial support by the MCIU of Spain (PID2020-113512GB-I00 and RED2018-102331-T) and the Comunidad de Madrid (S2018/NMT-4389) is acknowledged. C. N is indebted to Comunidad de Madrid for her predoctoral fellowship.

Keywords: differentiation · kinetic evolution ·pathway complexity · polymers · seeded self-assembly

[1] a) G. M. Whitesides, R. F. Ismagilov, *Science* **1999**, *284*, 89–92; b) J. F. Stoddart, *Nat. Chem.* **2009**, *1*, 14–15; c) E. Mattia, S. Otto, *Nat. Nanotechnol.* **2015**, *10*, 111–119.

[2] a) J. Matern, Y. Dorca, L. Sánchez, G. Fernández, *Angew. Chem. Int. Ed.* **2019**, *58*, 16730 –16740; *Angew. Chem.* **2019**, *131*, 16884 –16895; b) A. Sorrenti, J. Leira-Iglesias, A. J. Markvoort, T. F. A. de Greef, T. M. Hermans, *Chem. Soc. Rev.* **2017**, *46*, 5476–5490.

[3] a) T. F. A. de Greef, M. M. J. Smulders, M. Wolffs, A. P. H. J. Schenning, R. P. Sijbesma, E. W. Meijer, *Chem. Rev.* **2009**, *109*, 5687–5754; b) M. Wehner, F. Würthner, *Nat. Rev.* **2019**, *4*, 38–53.

[4] S. Dhiman, S. J. George, *Bull. Chem. Soc. Jpn.* **2018**, *91*, 687–699.

[5] P. A. Korevaar, S. J. George, A. J. Markvoort, M. M. J. Smulders, P. A. J. Hilbers, A. P. H. J. Schenning, T. F. A. de Greef, E. W. Meijer, *Nature* **2012**, *481*, 492–496.

[6] S. Ogi, K. Sugiyasu, S. Manna, S. Samitsu, M. Takeuchi, *Nat. Chem.* **2014**, *6*, 188-195.

[7] a) J. Kang, D. Miyajima, T. Mori, Y. Inoue, Y. Itoh, T. Aida, *Science*, **2015**, *349*, 646-651; b) R. D. Mukhopadhyay, A. Ajayaghosh, *Science*, **2015**, *349*, 241-242; c) S. Ogi, V. Stepanenko, K. Sugiyasu, M. Takeuchi, F. Würthner, *J. Am. Chem. Soc.* **2015**, *137*, 3300-3307; d) E. E. Greciano, L. Sánchez, *Chem. Eur. J.* **2016**, *22*, 13724–13730; e) E. E. Greciano, B. Matarranz, L. Sánchez, *Angew. Chem. Int. Ed.* **2018**, *57*, 4697–4701; *Angew. Chem.* **2018**, *130*, 4787–4791; f) H. Wang, Y. Zhang, Y. Chen, H. Pan, X. Ren, Z. Chen, *Angew. Chem. Int. Ed.* **2020**, *59*, 5185–5192. *Angew. Chem.* **2020**, **132**, 5223-5230.

[8] T. Fukui, S. Kawai, S. Fujinuma, Y. Matsushita, T. Yasuda, T. Sakurai, S. Seki, M. Takeuchi, K. Sugiyasu, *Nat. Chem.* **2017**, *9*, 493–499.

[9] A. Aliprandi, M. Mauro, L. de Cola, *Nat. Chem.* **2016**, *8,* 10–15.

[10] M. Wehner, M. I. S. Röhr, M. Böhler, V. Stepanenko,W. Wagner, F. Würthner, *J. Am. Chem. Soc.* **2019**, *141*, 6092–6107.

[11] E. E. Greciano, J. Calbo, E. Ortí, L. Sánchez, *Angew. Chem. Int. Ed.* **2020**, *59*, 17517–17524; *Angew. Chem.* **2020**, *132*, 17670-17677.

[12] a) S. Ghosh, X.-Q. Li, V. Stepanenko, F. Würthner, *Chem.—Eur. J.* **2008**, *14*, 11343-11357; b) S. Ogi, V. Stepanenko, J. Thein, F. Würthner, *J. Am. Chem. Soc.* **2016**, *138*, 670-678; c) E. E. Greciano, S. Alsina, G. Ghosh, G. Fernández, L. Sánchez, *Small Methods* **2020**, *4*, 1900715; d) E. E. Greciano, M. A. Martínez, S. Alsina, A. Laguna, L. Sánchez, *Org. Chem. Front.,* **2021**, *8*, 5328–5335.

[13] M. A. Martínez, A. Doncel-Giménez, J. Cerdá, J. Calbo, R. Rodríguez, J. Aragó, J. Crassous, E. Ortí, L. Sánchez, *J. Am. Chem. Soc.* **2021**, *143,* 13281−13291.

[14] D. S. Philips, K. K. Kartha, A. Politi, T. Krügger, R. Q. Albuquerque, G. Fernández, *Angew. Chem. Int. Ed.,* **2019**, *58*, 4732-4736; *Angew. Chem.* **2019**, *131*, 4782-4787.

[15] J. Matern, I. Maisuls, C. A. Strassert, G. Fernández, *Angew. Chem. Int. Ed.,* **2022**, *61*, e202208436; *Angew. Chem.* **2022**, *134*, e202208436.

[16] F. Würthner, C. R. Saha-Möller, B. Fimmel, S. Ogi, P. Leowanawat, D. Schmidt, *Chem. Soc. Rev.* **2016**, *116*, 962 –1052.

[17] F. Würthner, T. E. Kaiser, C. R. Saha-Möller, *Angew. Chem. Int. Ed.* **2011**, *50*, 3376–3410; *Angew. Chem.* **2011**, *123*, 3436-3473

[18] a) N. J. Hestand, F. C. Spano, *J. Chem. Phys.* **2015**, *143*, 244707; b) Y. Hong, J. Kim, W. Kim, C. Kaufmann, H. Kim, F. Würthner, D. Kim, *J. Am. Chem. Soc.* **2020**, *142*, 7845−7857.

[19] N. J. Hestand, F. C. Spano, *Acc. Chem. Res.* **2017**, *50*, 341−350

[20] H. M. M. ten Eikelder, A. J. Markvoort, T. F. A. de Greef, P. A. J. Hilbers, *J. Phys. Chem. B* **2012**, *116*, 5291–5301.

Entry for the Table of Contents

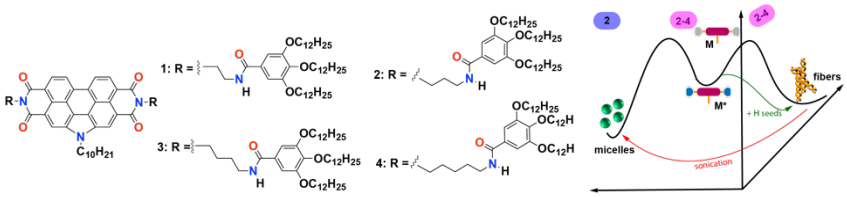

The self-assembly of N-annulated perylene bisimides (N-PBIs) has demonstrated that the ability of these units to generate different polymorphs upon supramolecular polymerization decreases as the length of the alkyl bridge separating the peripheral side chains and the central aromatic backbones decreases. The kinetically controlled supramolecular polymerization of these N-PBIs has also been investigated.

Institute and/or researcher Twitter usernames: @LSM_LAB; @quimicasUCM